Biosensors and Bioelectronics 24 (2009) 2458–2464

Contents lists available at ScienceDirect

Biosensors and Bioelectronics

journal homepage: www.elsevier.com/locate/bios

A multiple-ligand approach to extending the dynamic range of analyte quantification in protein microarrays

Olof Andersson, Henrik Nikkinen, Daniel Kanmert, Karin Enander *

Division of Sensor Science and Molecular Physics, Department of Physics, Chemistry and Biology, Linköping University, SE-581 83 Linköping, Sweden

ARTICLE INFO

Article history:
Received 10 November 2008
Received in revised form 16 December 2008
Accepted 17 December 2008
Available online 25 December 2008

Keywords:
Imaging surface plasmon resonance
Biosensor
Affinity microarray
Analyte quantification
Synthetic polypeptide

ABSTRACT

This work describes a concept for extending the dynamic range of quantification in an affinity biosensor assay by using a set of ligands with different affinities toward a common analyte. Three synthetic, biotinylated polypeptides capable of binding a model protein analyte with different affinities (10^{-9} M $\leq K_d \leq 10^{-7}$ M) were immobilized in a microarray format on a gold slide covered with an oligo(ethylene glycol)-containing alkane thiolate self-assembled monolayer. A five-element affinity array, comprising single-peptide spots as well as spots where peptides were immobilized in mixtures, was realized by means of piezodispensation. Imaging surface plasmon resonance was used to study binding of the analyte to the different spots. The lower limit of analyte quantification was ~3 nM and the corresponding upper limit was increased by more than an order of magnitude compared to if only the highest affinity ligand would have been used. Affinity array sensors with multiple ligands for each analyte are particularly interesting for omitting dilution steps and providing highly accurate data in assays where several analytes such as disease biomarkers with extremely variable concentrations are quantified in parallel.

1. Introduction

The protein microarray format has emerged as a highly promising concept for multiplexed, fast, inexpensive and automated protein expression profiling, functional characterization and biomarker screening, requiring a minimal amount of sample (Cretich et al., 2006; Seidel and Niessner, 2008; Templin et al., 2002; Zhu and Snyder, 2003). A typical microarray can be viewed as a set of miniaturized, parallel affinity biosensors where recognition elements (ligands) immobilized in discrete spots specifically capture the analytes of interest and allow their quantification. Any given ligand limits the dynamic range of analyte quantification to about two orders of magnitude, since the most reliable analysis is obtained when the analyte concentration is within 0.1–10 times the value of the equilibrium dissociation constant K_d of the interaction (Lakowicz, 2007). For each sample, the suitable ligand affinity is thus defined from the expected analyte concentration. In blood plasma, a sample matrix where many relevant protein analytes are found, concentrations of different proteins span at least ten orders of magnitude, albumin being the most abundant at 10^{-4} M (Anderson and Anderson, 2002). Also, the circulating concentration of disease biomarkers can vary tremendously between individuals and in response to disease-dependent stimuli. For example, serum levels of alpha-fetoprotein, a well-established marker for several carcinomas, may rise more than a thousand-fold in affected adults compared to normal values (Fujioka et al., 2001; Matsunou et al., 1994), while levels of C-reactive protein can increase more than ten thousand times upon acute inflammation (Pepys and Hirschfield, 2003). Traditionally, this calls for laborious sample preparation including systematic dilution in order to bring the analyte within the concentration window where reliable quantification is possible. An interesting strategy to extend the dynamic range of quantification, thus allowing for a more straightforward analysis, involves the simultaneous exposure of the sample to a set of ligands with different affinities for the analyte. This approach would be particularly relevant in large-scale analyses, such as expression profiling for diagnostics and monitoring, where several markers are quantified in parallel.

Synthetic polypeptides constitute an attractive class of molecules to be used as ligands in affinity microarrays. They can be straightforwardly and inexpensively produced with well-established methods, and in contrast to most full-length proteins such as antibodies, they provide excellent functional stability and are readily targeted for site-specific modifications in order to allow for, e.g., controlled immobilization or labeling. In this work, we present the design, manufacture and functional evaluation of an affinity array where synthetic peptides recognizing an antibody fragment with widely different affinities (10^{-9} M $\leq K_d \leq 10^{-7}$ M) were used as ligands. A microarray scaffold was created by microcontact printing of a biotin derivative

* Corresponding author. Tel.: +46 13 282359; fax: +46 13 288969.
E-mail address: karen@ifm.liu.se (K. Enander).

0956-5663/$ – see front matter © 2008 Elsevier B.V. All rights reserved.
doi:10.1016/j.bios.2008.12.030

onto a pre-activated self-assembled monolayer of oligo(ethylene glycol)-containing alkane thiolates on gold (OEG-SAM), followed by immobilization of neutravidin. Biotin-tagged peptides were piezodispensed into the predefined array spots and imaging surface plasmon resonance (iSPR) was employed as a label-free method of detection to study the response pattern of the array when the antibody fragment was introduced in solution. SPR is a very well established technique that allows for real-time analyses of biological interactions (Homola, 2008) and, when combined with surface patterning and applied in imaging mode, is particularly suitable for monitoring binding events to protein microarrays (Shumaker-Parry and Campbell, 2004; Wegner et al., 2004) or in high-throughput affinity studies (Rich et al., 2008; Wassaf et al., 2006).

2. Materials and methods

2.1. Polypeptide synthesis

Fab57P was expressed and affinity purified as described elsewhere (Enander et al., 2008). The peptides P1, corresponding to amino acids 134–151 of the tobacco mosaic virus coat protein with an additional biotinylated N-terminal glutamic acid residue (sequence: CH_3CO-E^{Bio}RGTGSYNR<u>SS</u>FES<u>SS</u>GLV-$CONH_2$), P2 (CH_3-CO-E^{Bio}KSYNR<u>SS</u>FETNSGLT-$CONH_2$), P3 (CH_3CO-E^{Bio}NKTSFSPP-PLSI-$CONH_2$), and P4 (CH_3CO-E^{Bio}RGSGTRSYSNEGF<u>SS</u>LSV-$CONH_2$) were synthesized on the solid phase using standard fluorenylmethoxycarbonyl (Fmoc) chemistry. A detailed description of the synthesis procedure is given as Supplementary information (S1). A biotin tag was introduced in the peptide N termini via a modified glutamic acid residue (E^{Bio}, from Fmoc-N-γ-(N-biotinyl-3-(2-(2-(3-aminopropyloxy)-ethoxy)-ethoxy)-propyl)-L-glutamine).
In the synthesis of P1, P2 and P4, a pseudoproline dipeptide, Fmoc-Ser(tBu)-Ser($\psi^{Me,Me}$pro)-OH, was used in some positions (underlined) instead of the amino acid form of Ser in order to improve yields. Peptides were cleaved from the solid phase by treatment with 95% trifluoroacetic acid (TFA), purified by reversed-phase HPLC and identified by MALDI-TOF mass spectrometry.

2.2. Kinetic analysis

For affinity determination, the peptides P1, P2 and P3 were synthesized without the biotin tag and with the N-terminal amino group available for immobilization. Also, slight sequence modifications were introduced in the N-terminal regions (P1: H_2N-RGTGSYNRSSFESSSGLV-$CONH_2$; P2: H_2N-RSYNRSSFETNSGLT-$CONH_2$; P3: H_2N-RNRTSFSPPPLSI-$CONH_2$). Kinetic analysis was performed using a Biacore 3000 instrument (GE Healthcare) operating at 25 °C. The polypeptides were immobilized in different flow channels on a dextran-coated CM5 chip employing conventional carbodiimide coupling chemistry (details are given as Supplementary information, S2). HEPES-buffered saline (HBS-EP: 10 mM HEPES, 0.15 M NaCl, 3 mM EDTA, 0.005% polysorbate 20, pH 7.4) was used as running buffer during the analysis. Fab57P dissolved to six different concentrations in the range 1.5–100 nM in HBS-EP was introduced at 50 μL/min during 2 min. The precise peptide concentrations are indicated in Fig. 2. The surface was efficiently regenerated with 50 mM HCl (30 s) after each analyte injection. Data analysis was performed using the BIAevaluation 4.1 software, by fitting data from the injection phase and the first 90 s of the post-injection phase using a 1:1 Langmuir bimolecular binding model in a global fit algorithm. All buffer solutions, chips and reagents were provided by GE Healthcare.

2.3. Immobilization and array manufacture

Gold-coated glass slides (kindly provided by GE Healthcare) were cleaned in a 5:1:1 mixture of Milli-Q water, 30% hydrogen peroxide and 25% ammonia for 10 min at 85 °C and immersed in a 5:1 mixed solution of 100 μM (total concentration) $HS(CH_2)_{11}CONH(C_2H_4O)_{10}(CH_2)_2OCH_3$ (mOEG) and $HS(CH_2)_{11}CONH(C_2H_4O)_{12}(CH_2)_2COOH$ (aOEG) (Polypure AS) in 99.5% ethanol at room temperature for a minimum of 24 hours. Reactive succinimide esters were introduced to the aOEG thiols by covering the substrates with an aqueous mixture of 0.05 M N-hydroxysuccinimide (NHS) and 0.2 M N-ethyl-N′-[3-(dimethylamino)-propyl]carbodiimide (EDC) for 20 min. Patterning of the substrates was achieved through microcontact printing. Poly(dimethylsiloxane) (PDMS) stamps with a grid pattern of 250 μm × 250 μm protruding squares (spacing: 250 μm) were molded on a silica master. Stamps were oxidized by exposure to air plasma (100 W, 0.02 mbar, 1 min) and immediately inked with 20 mM (+)-biotin-$(PEO)_3$-amine (Molecular Biosciences) in 99.5% ethanol, carefully dried under a stream of nitrogen gas and brought in conformal contact with the substrates during 5 min. Substrates were then immersed in buffer (HBS-EP, GE Healthcare) for 20 min to allow for dissociation of non-covalently adsorbed biotin-$(PEO)_3$-amine, followed by incubation with 1.7 μM neutravidin (Pierce) in HBS-EP containing 1% (w/v) trehalose (see remarks in Supplementary information, S3) in a high humidity atmosphere for 2 h. Peptide solutions were delivered to different array elements by means of piezodispensation using a dispenser from Microdrop Technologies, Germany (see Section S3 in Supplementary information for technical details). Solutions of biotinylated peptides (total concentration: 200 μM) were prepared in trehalose-containing HBS-EP. Dispensation was performed at elevated humidity (70–80% RH) while simultaneously cooling the substrates to dew-point temperature to prevent evaporation. In addition to the individual polypeptides P1, P2 and P3, equimolar mixtures of P1 + P2 and P2 + P3 were also included. The affinity arrays were dispensed in pentuplicates on each substrate surface. Substrates were then drenched in 200 μM biotinylated P4 during 30 min in order to block any remaining binding sites on neutravidin. The peptide arrays were studied with iSPR immediately after fabrication.

2.4. Imaging surface plasmon resonance measurements

The iSPR measurements were performed using a custom-built instrument based on spectral interrogation in the Kretschmann configuration (Fig. 1). The iSPR instrument comprised two motorized goniometers (RV160, Newport Inc.) with synchronously movable arms, enabling an arbitrary choice of incidence angle. Surface plasmons were excited by means of an equilateral prism (BK7 glass) to which the substrate surfaces were optically coupled using a refractive index matching oil (n = 1.517, Cargille Inc.). Light passed through a monochromator (SpectraPro 300i, Acton Research Corp.) was collimated and polarized before being guided towards the prism by means of mirrors mounted on one of the movable arms. The grating density was 300 mm^{-1} and the wavelength interval was 650–760 nm. A CCD detector (Retiga Exi, QImaging Corp.) and imaging optics was mounted on the opposite movable arm. Here, the angle of incidence was fixed at 70°, where one pixel of the CCD detector depicted an area of 2.2 μm × 5.8 μm. A flow cell (5 mm × 5 mm × 0.1 mm) was used to inject samples over the SPR surfaces. A continuous flow of buffer (30 μL/min) was maintained between and during sample injections. During measurements in kinetic mode, the wavelength was fixed at 685 nm and the mean reflectivity of TM-polarized light from each element in the array was monitored as a function of time. In addition,

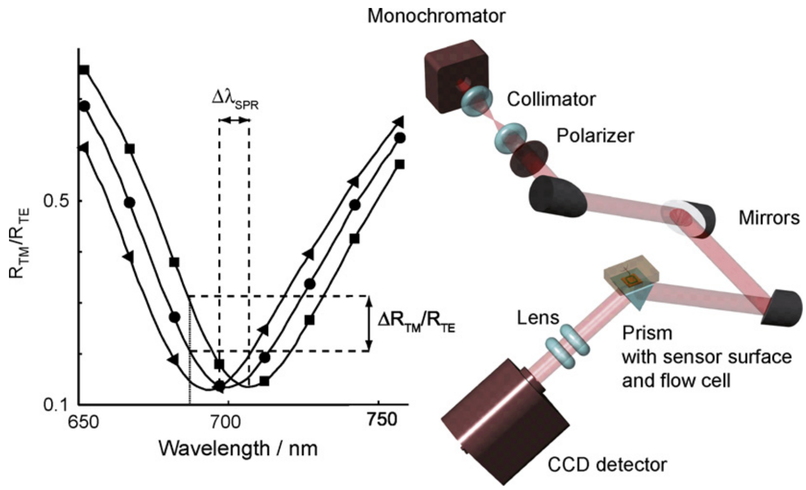

Fig. 1. Experimental reflectivity curves acquired from an OEG-SAM barrier region (triangles) and an array spot containing P1 before (circles) and after (squares) injection of Fab57P. The two parameters measured in this paper – the change in reflectivity ($\Delta R_{TM}/R_{TE}$) and the change in SPR wavelength ($\Delta\lambda_{SPR}$) – are indicated in the graph. A cartoon of the iSPR instrumental setup is also shown.

SPR surface maps were created by scanning the wavelength and determining λ_{SPR}, which is the wavelength where the reflectivity of TM-polarized light is at a minimum. In order to account for the wavelength dependence in the monochromator efficiency and detector sensitivity, the reflectivity of TE-polarized light was used for normalization. The SPR wavelength was determined using a weighted centroid algorithm (Johansen et al., 2000). In order to reduce noise, only reflectivity values below 60% were included in the λ_{SPR} calculations. No noise reduction was performed in kinetic mode, except averaging over as large an area as possible (approximately 200 μm × 200 μm). The maximal response was determined by averaging over a period of 5 s at the peak of the injection. The sample speed was 4 Hz and SPR maps comprising data from a full wavelength scan could be acquired at a rate of 1 min^{-1}. Samples of Fab57P were injected during 4.5 min and the post-injection phase was monitored for at least 4 min. Regeneration was efficiently achieved by two subsequent 45 s injections of 10 mM glycine-HCl pH 2.5 (GE Healthcare).

3. Results and discussion

3.1. Biomolecular model system

The affinity array was based on a set of synthetic polypeptides binding to the recombinant antibody fragment Fab57P (Chatellier et al., 1996) with different affinities. Fab57P recognizes the 18 kDa tobacco mosaic virus coat protein (TMVP) and a peptide corresponding to TMVP residues 134–151 with similar affinities (Choulier et al., 1999). The kinetic parameters describing the interaction between the TMVP-derived peptide (here denoted P1) and Fab57P have been determined, giving K_d = 1.8 and 1.6 nM. (Choulier et al., 2001; Enander et al., 2008) P1 was employed as the highest affinity recognition molecule in the array. The second peptide, P2, was rationally designed by deleting three N-terminal amino acids in P1 and exchanging Ser146 for Thr, Ser147 for Asn, and Val151 for Thr. Individually, these or similar modifications in P1 affect the affinity toward Fab57P only marginally (Choulier et al., 2001), but when performed in concert they were expected to significantly increase K_d while still retaining it in the medium nanomolar range. The sequence of the third peptide, P3, was originally identified in a phage display study where it was reported to bind Fab57P with K_d = 0.36 μM (Choulier et al., 2001). A fourth peptide, P4, corresponding to a scrambled sequence of P1 and expected not to bind Fab57P, was included to block non-occupied neutravidin binding sites after immobilization of P1, P2 and P3 to the array.

3.2. Affinity of the polypeptides for Fab57P

Conventional, non-imaging SPR (Biacore) was employed in order to determine the association (k_a) and dissociation (k_d) rate constants describing the interactions of P1, P2 and P3 with Fab57P. SPR responses upon introduction of Fab57P at different concentrations to peptides immobilized in a dextran hydrogel are shown in Fig. 2. From fitting of a Langmuir 1:1 bimolecular binding model to the experimental data, K_d was found to be 0.95, 13 and 370 nM for P1, P2 and P3, respectively (Table 1). Affinities of P1 and P3 determined in earlier studies (Choulier et al., 2001) were thus largely confirmed. As P2 was newly designed and had not been characterized before, the kinetic analysis with this peptide was performed three times with independent peptide immobilizations and resulted in K_d = 13, 13 and 15 nM. This decrease in affinity relative to P1 was due to a large increase in k_d, while k_a was unchanged. The goodness of fit was assessed by inspection of the residual plots and by relating the average squared residuals, χ^2, to the experimental value of the maximum SPR response, $R_{max,\,exp}$. In all cases, the fitted curves agreed very closely with the experimental data and statistical parameters were excellent with a $\chi^2/R_{max,\,exp}$ ratio of ≤0.02. While the kinetic analysis was carried out with peptides immobilized on a three-dimensional hydrogel surface, it was assumed that affinities were affected only marginally by the different immobilization method and surface design used in the microarray experiments. At the conditions used for the interaction analysis of P1, P2 and P3, there were no detectable interactions between P4 and Fab57P (see Section S2 in Supplementary information).

3.3. Surface design and immobilization

A prerequisite for successful interaction analysis in affinity biosensors is negligible non-specific binding of the analyte and/or other sample components to the background. Accordingly, we employed a surface chemistry based on alkane thiols with ethylene glycol tail groups, which are known to suppress protein adsorption when forming SAMs on gold (Prime and Whitesides, 1991). Furthermore, in any surface-based biosensor system, functionality and reproducibility depend critically on the ability to achieve controlled immobilization levels of the ligand. This is particularly important in affinity biosensors, since the analyte binding capacity

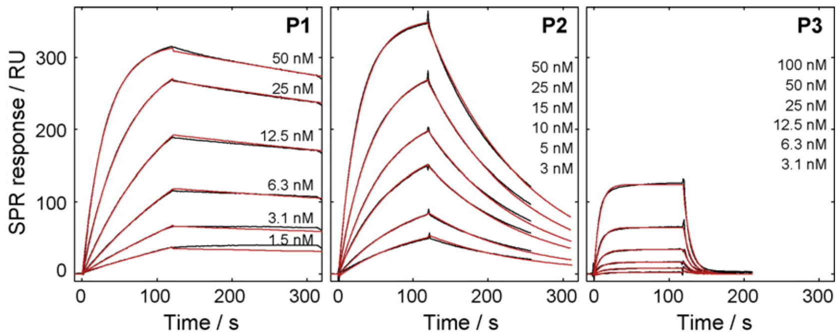

Fig. 2. Sensorgrams reflecting the interaction between Fab57P at indicated concentrations and immobilized peptides P1, P2, and P3 (black curves). Curves obtained from a global fit algorithm and used for the determination of kinetic parameters are shown in red. (For interpretation of the references to color in this figure legend, the reader is referred to the web version of the article.)

Table 1
Kinetic parameters for the interaction between Fab57P and the peptides P1, P2 and P3.

Peptide	Level of immobilization[a] (RU)	$R_{max, exp}$[b] (RU)	k_a, (10^5 M^{-1}s^{-1})	k_d, (10^{-4} s^{-1})	K_d, (10^{-9} M)	χ^2 (RU^2)	$\chi^2/R_{max, exp}$ (RU)
P1	20	320	6.4	6.1	0.95	6.8	0.021
P2	49	430	5.8	76	13	2.4	0.0056
P3	39	560	2.8	1040	370	2.2	0.0039

[a] The level of immobilization is defined as the difference in baseline before and immediately after injection of the peptide.
[b] $R_{max, exp}$ as obtained from the global fit.

is a function of the ligand surface concentration as well as of the interaction kinetics. Specifically, if the ligands of an affinity array are immobilized at equal levels, and if they are equally accessible to binding, then the equilibrium concentrations of the ligand–analyte complex formed in each spot upon exposure to the sample will be different and can be monotonically related to the affinities. This allows for straightforward interpretation of the array response pattern.

In the initial immobilization approach, peptide variants identical to those used for affinity analysis (with the N-terminal amino group available for immobilization) were covalently coupled by means of piezodispensation to an OEG-SAM formed by a mixture of carboxyl-

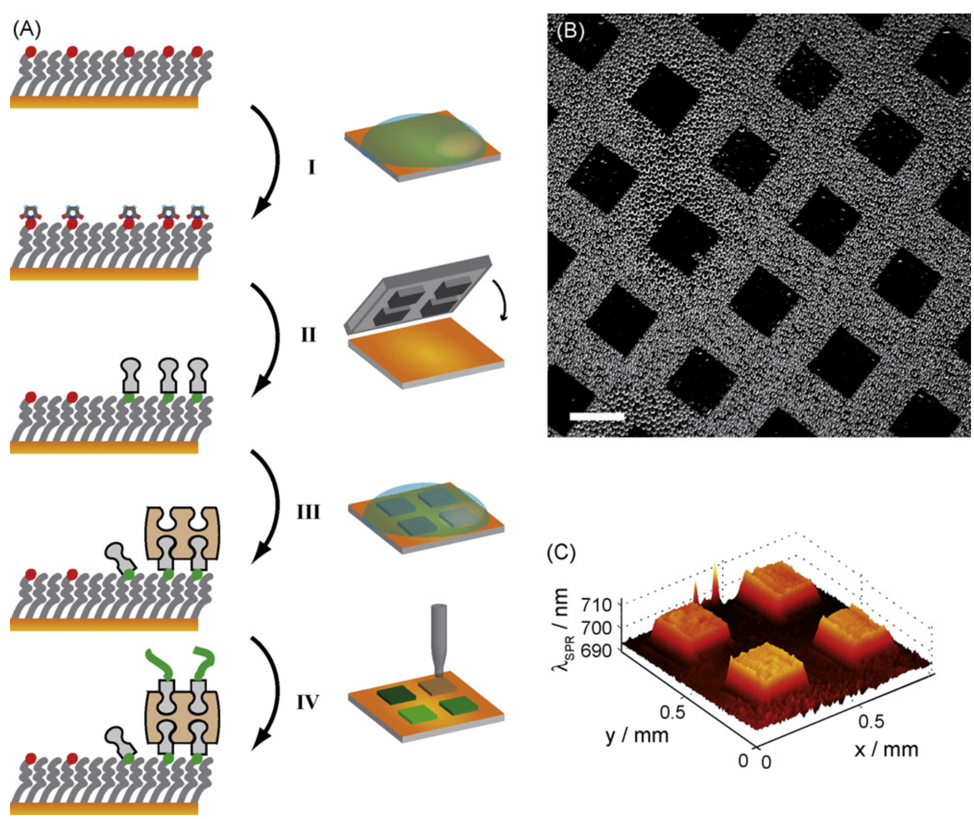

Fig. 3. Array manufacture. (A) Starting with a mixed OEG-SAM, the different steps of manufacture are activation with EDC/NHS (I), microcontact printing of a biotin derivative (II), incubation with neutravidin (III), and piezodispensation of polypeptides (IV). A micro-wetting image and an iSPR map of a neutravidin array after step III in the manufacture process are shown in (B) and (C), respectively. The hydrophilic neutravidin spots are completely covered with water and appear dark (B), while only tiny water droplets have condensed on the hydrophobic mOEG/aOEG SAM barriers. The scalebar is 250 μm.

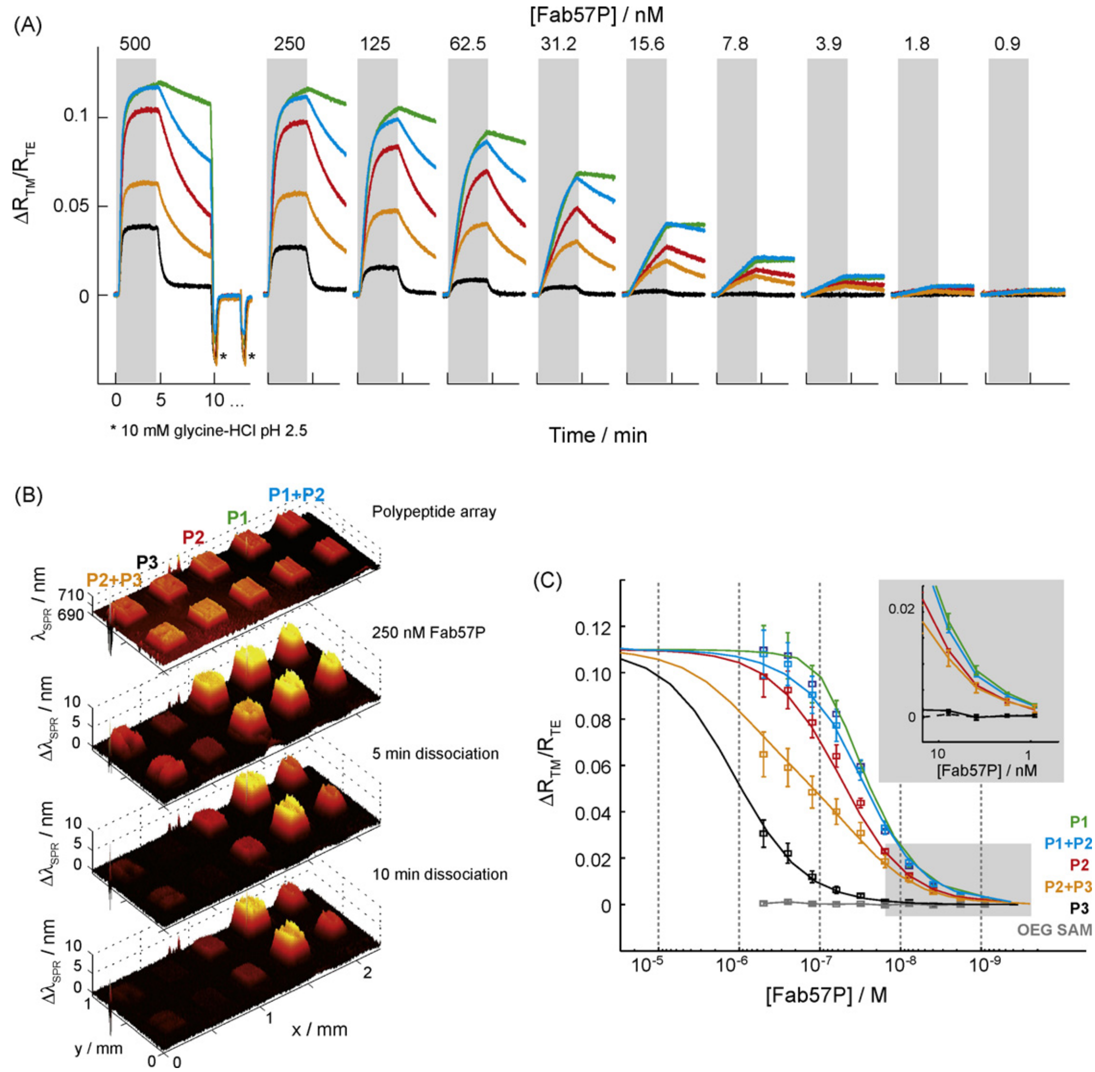

Fig. 4. Interaction monitoring using iSPR. (A) Sensorgrams showing the shift in reflectivity upon injection of Fab57P (different concentrations in random order) of each of the unique spots in the array, monitored during the injection (shaded) and post-injection phases. The intermediate regeneration steps are shown only for the first injection. (B) SPR wavelength maps showing the shift in λ_{SPR} upon introduction of 250 nM Fab57P to two affinity arrays in parallel comprising P1 (green), P2 (red), P3 (black), P1 + P2 (blue) and P2 + P3 (orange). (C) Calibration curves for each polypeptide element of the array (squares). The gray curve shows lack of non-specific binding of Fab57P to the OEG-SAM. The error bars show the experimental standard deviation determined from the replicate spots. The solid lines in the full graph represent fits obtained under the assumption that the peptide immobilization levels are equal in all spots, and are included as guides. (For interpretation of the references to color in this figure legend, the reader is referred to the web version of the article.)

terminated and methoxy-terminated thiols, following activation of the carboxyl groups. It was found that under similar conditions, the immobilization capacity of the peptides was very different and difficult to control (data not shown). Therefore, we next opted for a tag-mediated immobilization approach where a neutravidin linker layer was introduced to the substrate. The peptides were resynthesized with an N-terminal biotin tag, expecting that the extremely high affinity between biotin and neutravidin would overrule any sequence-intrinsic immobilization propensities. The steps in the array manufacture based on biotin–neutravidin coupling are outlined in Fig. 3A. The carboxyl groups of the aOEG thiolates in the SAM were activated by covering the surface with EDC/NHS (Step I). A biotin derivative containing a primary amino group was introduced through microcontact printing (Step II) (Lahiri et al., 1999). Following incubation in neutravidin (Step III), P1, P2, and P3 as well as equimolar mixtures thereof (P1 + P2 and P2 + P3) were delivered to the surface through piezodispensation (Step IV). Peptides were dispensed at high concentrations (200 μM) in order to approach saturation of the binding sites. The level of immobilization was thus governed by the surface concentration of neutravidin, which was assumed to be uniform in each spot. There are some key advantages of this surface patterning approach. Firstly, SAMs exposing hydrophilic tail-groups typically cause droplets to spread over the surface during piezodispensation, increasing the risk of cross contamination between neighboring spots in an array. By using a mixed SAM, wherein a methoxy-terminated thiolate is a large constituent, the surface energy is lowered, leading to less spreading of droplets. Furthermore, after patterning with biotin and neutravidin, the array spots are more hydrophilic than the surrounding SAM. This is illustrated in the micro-wetting image of Fig. 3B, where the neutravidin spots are completely covered with water, whereas only tiny droplets have formed on the SAM. In this way, the hydrophilic neutravidin spots serve to confine the ligand droplets during dispensation. In Fig. 3C, an SPR wavelength map of four elements of the array surface in Fig. 3B is shown. A qualitative, iSPR-based evaluation of the immobilization levels (a detailed analysis was precluded by the limited sensitivity of the instrument) indicated that the surface concentrations of the different peptides were considerably more similar than those obtained when using direct amine coupling. Indirectly, this was also confirmed by the

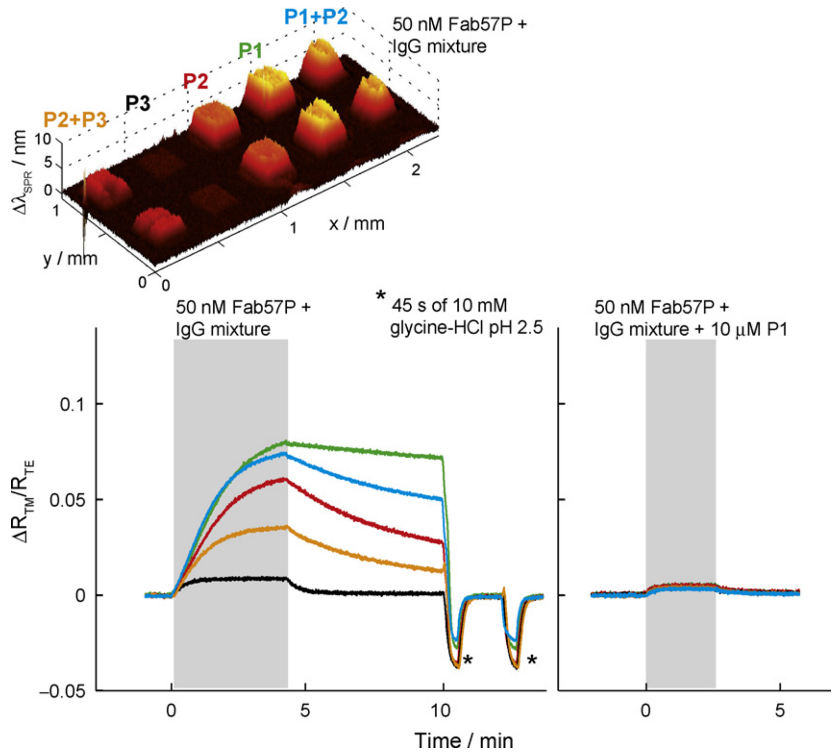

Fig. 5. SPR response upon injection of 50 nM Fab57P together with a mixture of IgGs. The regeneration step and a control experiment are also shown where 10 μM P1 was added to the sample to inhibit the interaction.

response of the array elements to Fab57P, decreasing in the order P1 > P2 > P3 (Fig. 4A).

3.4. Array evaluation by iSPR

In order to demonstrate the concept of immobilized affinity arrays that allow for an extensive dynamic range of analyte quantification, the array response upon introduction of Fab57P at different concentrations (1–500 nM) was monitored using iSPR. Sensorgrams showing the SPR response as a function of time at each array spot with Fab57P at different concentrations are plotted in Fig. 4A. Two short pulses of 10 mM glycine-HCl pH 2.5 efficiently regenerated the surface with maintained interaction capacity (shown for the first injection only in Fig. 4A). The SPR maps in Fig. 4B show the shift in SPR wavelength of each spot on the array before, during and after injection of 250 nM Fab57P. Each spot exhibits a unique response pattern to the analyte, which is particularly evident when studying the post-injection phase where the ligand–analyte complexes dissociate at different rates.

Calibration curves were constructed by averaging the SPR response from five different arrays on one substrate surface after exposure to Fab57P during 4.5 min (Fig. 4C). The length of the error bars is two standard deviations. The lower limit of detection, taken as the standard deviation of the baseline noise during continuous flow of buffer multiplied by three, was assessed at ∼1 nM, corresponding to an SPR response of $\Delta R_{TM}/R_{TE} = 0.001$. Similarly, the lower limit of quantification, taken as the standard deviation of the baseline noise multiplied by ten, was ∼3 nM. These values were extracted from responses of the P1-containing spots. The fact that K_d of the P1-Fab57P interaction is close to 1 nM indicates that from a biochemical point of view, concentrations of Fab57P even lower than 3 nM should be possible to determine. However, with the experimental setup used here, instrument parameters rather than biochemical principles determine the actual lower limit of detection. Provided there are still available immobilization sites, increasing the surface concentration of the ligands would be a means to lower this limit further.

Fig. 4C shows that the highest affinity spots, P1 and P1 + P2, approach saturation as the Fab57P concentration enters the μM regime. However, at these analyte concentrations, the lower affinity spots P3 and P2 + P3 provide maintained sensitivity and are useful for quantification. The upper limit of quantification could not be determined due to limited availability of the analyte, but was estimated to be increased by more than an order of magnitude compared to if only P1 would have been used. For the same reason, the injection phase was limited to 4.5 min, and equilibrium binding levels could not be fully reached. Importantly, no non-specific binding of Fab57P to the OEG-SAM surrounding the spots of the array was observed (gray curve).

While the affinity array in this model system only comprise three unique polypeptide sequences, by mixing the peptides, array elements exhibiting different binding characteristics could be created. Qualitatively, a peptide mixture exhibits an apparent K_d between those of the peptides that the mixture is composed of. Thus, calibration curves obtained from "mixed spots" (P1 + P2, P2 + P3) ran nicely between those obtained from the corresponding single-peptide spots. Mixing the ligands does not increase the dynamic range of quantification and could be considered analogous to dilution followed by a mere averaging of the response from the single-peptide spots. However, the mixed spots do provide additional response values which could be used in fitting of experimental data and allow for a more reliable concentration determination as compared to when having only fewer measured values at disposal. As indicated by the shape of the calibration curve of P2 + P3, a large dynamic range affinity sensor could be constructed without the need for addressing individual spots, by mixing ligands of different affinities in one single area of detection. Such "composite biosensors" have been suggested previously in a solution-based approach (Marvin et al., 1997). In contrast, our array concept allows for analyte quantification by means of pattern recognition based on an arbitrary number of spots where unique fractional mixtures of different ligands are immobilized.

In order to further confirm the specificity of the polypeptide affinity array, a sample containing 50 nM Fab57P and a mixture of IgGs (1 μM) was introduced to the array. The response is illustrated in an SPR map and a sensorgram in Fig. 5, showing excellent agreement with the sensorgrams and calibration curves in Fig. 4. Thus, the presence of proteins with non-related binding specificity did not disturb the interaction of Fab57P with the array. Furthermore, the injection was repeated after addition of 10 μM P1 to the sample solution. As expected, the presence of P1 in large excess vis-à-vis Fab57P efficiently inhibited binding of the analyte to the spots of the affinity array. The small response that can be discerned is due to the difference in bulk refractive index during the injection caused by trehalose present in the P1-containing buffer solution.

In order to generalize the affinity array concept to target relevant analytes, finding ligands with desired affinities that remain functionally stable when immobilized will be a crucial issue. Classes of robust molecules suitable for ligand generation include nucleic acid aptamers selected from combinatorial libraries by selective evolution of ligands (SELEX) (Ellington and Szostak, 1990; Tuerk and Gold, 1990) and scFvs selected from recombinant antibody libraries (Steinhauer et al., 2002). In the model array presented here, synthetic polypeptides were used. Starting from a sequence that was well characterized with respect to binding of the analyte (P1), lower affinity ligands used in the array were obtained either by a rational design approach (P2) or a combinatorial method (P3). Traditionally, in the generation of recognition elements, there is a strong focus on designing or selecting those with the highest possible affinity toward the target. Naturally, these efforts will still be relevant in an affinity array context, since high-affinity ligands are needed to decrease the lower level of quantification. However, for high-abundance analytes, increasing the upper level of quantification may be equally important, requiring recognition elements with moderate affinities. In selection procedures, such ligands appear in parallel with the high-affinity ones and their generation does therefore not require additional efforts.

4. Conclusions

By controlled surface arraying of a set of functionally robust ligands with a wide range of affinities for a common analyte, we have demonstrated how the dynamic range of an analyte quantification assay can be extended beyond the two orders of magnitude typically obtained with a single ligand. The choice of immobilization strategy was found to be very important for array performance. With the model interaction system used here, the lower limit of analyte quantification was found to be ~3 nM, provided by the highest affinity ligand P1. While saturation of P1 was reached at ~200 nM, the response of the lowest affinity ligand P3 at this analyte concentration was only ~25% of its estimated maximum value. Moreover, the number of elements in the affinity array was increased by mixing the ligands, resulting in additional spots with unique response patterns and allowing for an even more accurate quantitative analysis. The affinity array concept is expected to become particularly useful in the multiplexed quantification of analytes present at different and highly variable concentrations.

Acknowledgements

During this work, K.E. was enrolled in the NanoSense programme, financed by the Swedish Foundation for Strategic Research. Financial support was further obtained from Carl Tryggers Stiftelse, Magn. Bergvalls Stiftelse, the Swedish Research Council and the European Commission through the Integrated Project “HealthCARE by Biosensor Measurements And Networking” (CAREMAN, NMP4-CT-2006-017333). The authors are grateful to Dr. Danièle Altschuh and Prof. Bo Liedberg for valuable discussions.

Appendix A. Supplementary data

Supplementary data associated with this article can be found, in the online version, at doi:10.1016/j.bios.2008.12.030.

References

Anderson, N.L., Anderson, N.G., 2002. Mol. Cell. Proteomics 1 (11), 845–867.
Chatellier, J., Rauffer-Bruyère, N., van Regenmortel, M.H.V., Altschuh, D., Weiss, E., 1996. J. Mol. Recognit. 9 (1), 39–51.
Choulier, L., Laune, D., Orfanoudakis, G., Wlad, H., Janson, J.C., Granier, C., Altschuh, D., 2001. J. Immunol. Methods 249 (1–2), 253–264.
Choulier, L., Rauffer-Bruyère, N., Ben Khalifa, M., Martin, F., Vernet, T., Altschuh, D., 1999. Biochemistry 38 (12), 3530–3537.
Cretich, M., Damin, F., Pirri, G., Chiari, M., 2006. Biomol. Eng. 23 (2–3), 77–88.
Ellington, A.D., Szostak, J.W., 1990. Nature 346 (6287), 818–822.
Enander, K., Choulier, L., Olsson, A.L., Yushchenko, D.A., Kanmert, D., Klymchenko, A.S., Demchenko, A.P., Mély, Y., Altschuh, D., 2008. Bioconjug. Chem. 19 (9), 1864–1870.
Fujioka, M., Nakashima, Y., Nakashima, O., Kojiro, M., 2001. Hepatology 34 (6), 1128–1134.
Homola, J., 2008. Chem. Rev. 108 (2), 462–493.
Johansen, K., Stalberg, R., Lundstrom, I., Liedberg, B., 2000. Meas. Sci. Technol. 11 (11), 1630–1638.
Lahiri, J., Ostuni, E., Whitesides, G.M., 1999. Langmuir 15 (6), 2055–2060.
Lakowicz, J.R., 2007. Principles of Fluorescence Spectroscopy, 3rd ed. Kluwer Academic/Plenum Publishers, New York.
Marvin, J.S., Corcoran, E.E., Hattangadi, N.A., Zhang, J.V., Gere, S.A., Hellinga, H.W., 1997. Proc. Natl. Acad. Sci. U.S.A. 94 (9), 4366–4371.
Matsunou, H., Konishi, F., Jalal, R.E.A., Yamamichi, N., Mukawa, A., 1994. Cancer 73 (3), 534–540.
Pepys, M.B., Hirschfield, G.M., 2003. J. Clin. Invest. 111 (12), 1805–1812.
Prime, K.L., Whitesides, G.M., 1991. Science 252 (5009), 1164–1167.
Rich, R.L., Cannon, M.J., Jenkins, J., Pandian, P., Sundaram, S., Magyar, R., Brockman, J., Lambert, J., Myszka, D.G., 2008. Anal. Biochem. 373 (1), 112–120.
Seidel, M., Niessner, R., 2008. Anal. Bioanal. Chem. 391 (5), 1521–1544.
Shumaker-Parry, J.S., Campbell, C.T., 2004. Anal. Chem. 76 (4), 907–917.
Steinhauer, C., Wingren, C., Hager, A.C.M., Borrebaeck, C.A.K., 2002. Biotechniques 33 (Suppl.), 38–45.
Templin, M.F., Stoll, D., Schrenk, M., Traub, P.C., Vohringer, C.F., Joos, T.O., 2002. Trends Biotechnol. 20 (4), 160–166.
Tuerk, C., Gold, L., 1990. Science 249 (4968), 505–510.
Wassaf, D., Kuang, G.N., Kopacz, K., Wu, Q.L., Nguyen, Q., Toews, M., Cosic, J., Jacques, J., Wiltshire, S., Lambert, J., Pazmany, C.C., Hogan, S., Ladner, R.C., Nixon, A.E., Sexton, D.J., 2006. Anal. Biochem. 351 (2), 241–253.
Wegner, G.J., Wark, A.W., Lee, H.J., Codner, E., Saeki, T., Fang, S.P., Corn, R.M., 2004. Anal. Chem. 76 (19), 5677–5684.
Zhu, H., Snyder, M., 2003. Curr. Opin. Chem. Biol. 7 (1), 55–63.